

Vibration-induced PM Noise in Oscillators and its Suppression

Archita Hati, Craig Nelson and David Howe
National Institute of Standards and Technology
USA

1. Introduction

High-precision oscillators have significant applications in modern communication and navigation systems, radars, and sensors mounted in unmanned aerial vehicles, helicopters, missiles, and other dynamic platforms. These systems must provide their required performance even when subject to mild to severe dynamic environmental conditions. Oscillators often can provide sufficiently low intrinsic phase modulation (PM) noise to satisfy particular system requirements when in a static environment. However, these oscillators are sensitive to acceleration that can be in the form of steady acceleration, vibration, shock, or acoustic pickup. In most applications the acceleration experienced by an oscillator is in the form of vibration, which can introduce mechanical deformations that deteriorate the oscillator's otherwise low PM noise (Filler, 1988; Vig et al., 1992; Howe et al., 2005). This degrades the performance of the entire electronic system that depends on this oscillator's low phase noise. For example, when radars and sensors mounted on helicopters are subjected to severe low- and medium-frequency vibration environments, the vibration noise induced into the system's reference oscillator translates to blurring of targets and possibly false detection.

This sensitivity to vibration originates most commonly from phase fluctuations within the oscillator's positive-feedback loop, due usually to the physical deformations in the frequency determining element, the resonator. Factors that lead to high acceleration sensitivity of the resonator include nonlinear or sensitive mechanical coupling effects and lack of mechanical symmetry that serve to cancel frequency changes in the resonator. Vibration also causes mechanical deformations in non-frequency-determining electronic components that then cause phase fluctuations (Steinberg, 2000). Because these fluctuations are inside the oscillator feedback loop and are integrated according to Leeson's model (Leeson, 1966), they can become large at Fourier, or offset, frequencies close to carrier frequency. An oscillator's sensitivity to vibration is characterized traditionally by acceleration sensitivity, which is the normalized frequency change per g (1 g is the acceleration of gravity near the earth's surface, approximately 9.8 m/s²). Typically, frequency shifts in oscillators are on the order of 10⁻⁸ to 10⁻¹⁰ per g, primarily because of the physical deformations.

Work of US Government, not subject to copyright. Commercial products are identified in this document only for complete technical description; no endorsement is implied.

Vibration-induced noise can be suppressed by physical means and further by electronic means if a suitably low-cost way of measuring and correcting the vibration-induced noise from an oscillator is implemented. Passive mechanical isolation systems consist of elastic and damping materials that translate vibration energy to different frequencies where they are less troublesome and/or damped (Renoult et al., 1989). Active mechanical systems use accelerometers and mechanical actuators to measure and cancel motion induced by the vibration. Hybrid active-passive systems allow higher degrees of vibration isolation to be achieved, but such systems are not easily miniaturized, are somewhat complex, and are power-consuming (Weglein, 1989). In principle, atom-based frequency-determining elements such as those used in atomic frequency standards have extremely low acceleration sensitivity (Thieme et al., 2004). However, the state-selection, RF interrogation, and detection electronics are more complex than in oscillators, and the corresponding large volume of atomic standards make them equally vulnerable to mechanical deformation under vibration. Some method of suppressing induced frequency shifts is often required to even approach 10^{-10} per g (Kwon & Hahn, 1983). More compact atomic standards allow for simpler mechanical vibration isolation to be incorporated (Riley, 1992).

Strategies for electronically reducing acceleration sensitivity have traditionally relied on accurately detecting this vibration with sensors (Healy et al., 1983) and even using the resonator itself as a vibration sensor (Watts et al., 1988). Suppression at one vibration frequency along one axis in quartz oscillators by electronic means has been explored with success (Rosati & Filler, 1981). More recently, significant advances have been made in which this electronic vibration suppression is effective over a wide range of vibration frequencies from a few hertz to 200 Hz. This is accomplished by fabricating high-Q quartz resonators in which the “cross” g-sensitivities of the three orthogonal axes are decoupled to a high degree (Bloch et al., 2006).

This chapter is intended to introduce the subject of vibration-induced PM noise by discussing the method of characterizing acceleration sensitivity and reporting such characterization on a sample of devices operating at microwave frequencies. Schemes for reducing vibration-induced noise are also discussed.

2. Defining Acceleration Sensitivity

If the vibration frequency from mechanical shock or other external processes is f_v , the vibration-induced phase fluctuations cause the carrier frequency to deviate from its nominal frequency, f_0 , by an amount $\pm \Delta f$ at a rate of f_v . Spurious sidebands, a highly undesirable type of noise in many applications, will appear at $f_0 \pm f_v$. The red curve in Figure 1 shows the PM noise of one test oscillator that is subjected to 100 Hz vibration along one axis. Note that the intrinsic random electronic noise is degraded by additional noise due to this vibration (shown as the noise pedestal on both sides of an ideal carrier signal). Also, the blue curve indicates that as the vibration increases, so do the sidebands, eventually exceeding the carrier power.

Low acceleration sensitivity at one frequency such as 100 Hz does not necessarily mean that phase noise due to acoustic and structure-borne vibration is suppressed. While vibration-induced noise modulation on an oscillator may be proportional to overall acceleration sensitivity, the proportionality as a function of f_v can be complicated in the range of audio frequencies of concern here (from a few Hertz to 2 kHz). Resonator deformations that affect its center frequency depend on designs of mounting, elastic properties of materials, acoustic

resonances, sound and vibration isolation, orientation, etc. Therefore, suppression of only “dc or time-independent” acceleration sensitivity due to what is commonly called 2 g-tipover (Vig et al., 1992) or steady acceleration has limitations and is insufficient to solve the larger problem of “ac or time dependent” acceleration sensitivity due to vibration. Acceleration sensitivity and vibration sensitivity are often used interchangeably for time-dependent accelerations. The acceleration sensitivity is characterized more fully as a function of f_v , as discussed next.

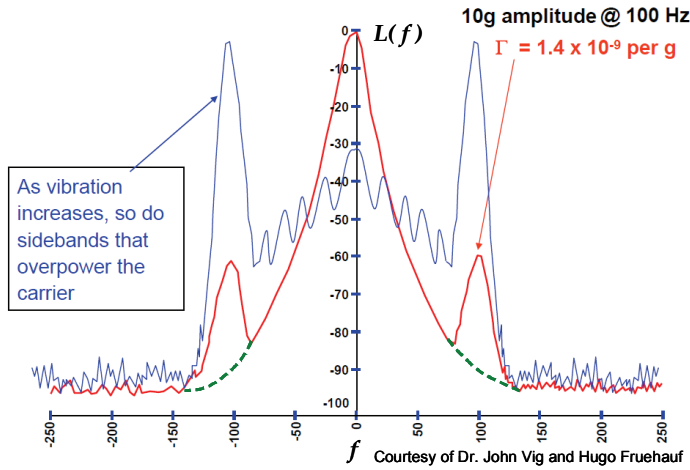


Figure 1. Phase noise of an oscillator that is subjected to vibration at $f_v = 100$ Hz. f is the offset frequency from the carrier

Acceleration sensitivity of an oscillator is explained in detail by Filler [Filler, 1988]. When an oscillator is subjected to acceleration, its resonant frequency shifts. The peak frequency shift Δf_{peak} , which is proportional to magnitude of the acceleration and dependent on the direction of acceleration, is given by a peak fractional-frequency change y_{peak} as

$$y_{peak} = \frac{\Delta f_{peak}}{f_0} = \bar{\Gamma} \cdot \bar{a}, \tag{1}$$

where f_0 is the frequency of the oscillator with no acceleration, $\bar{\Gamma}$ is the acceleration sensitivity vector and \bar{a} is the peak applied acceleration vector. The magnitude of acceleration is expressed in units of g. When the direction of acceleration is parallel to the axis of acceleration sensitivity vector, it will have the greatest effect on Δf_{peak} .

By definition, $S_y(f)$ is the power spectral density of root-mean-square (rms) fractional-frequency change, y_{rms} (Sullivan et al., 1990), and is given by

$$S_y(f) = \frac{|y_{rms}|^2}{BW} = \left| \frac{\Delta f_{rms}}{f_0} \right|^2 \frac{1}{BW} = \left| \frac{\Delta f_{peak}}{\sqrt{2} f_0} \right|^2 \frac{1}{BW} \quad [1/Hz], \tag{2}$$

where f is the offset, or Fourier, frequency away from the carrier and BW is the bandwidth of the spectral-density measurement. Also, $S_y(f)$ is related to power spectral density of phase fluctuations as

$$S_{\phi}(f) = S_y(f) \left(\frac{f_0}{f} \right)^2 \dots [\text{rad}^2/\text{Hz}], \quad (3)$$

and the single sideband PM noise $L(f)$ is defined as

$$L(f) \equiv \frac{1}{2} S_{\phi}(f) \quad [\text{dBc}/\text{Hz}], \quad (4)$$

where dBc/Hz is dB below the carrier in a 1 Hz bandwidth. Substituting $f = f_v$ the vibration frequency, and normalizing to a 1 Hz bandwidth, $L(f_v)$ can be related to acceleration sensitivity for a small modulation index as

$$\begin{aligned} L(f_v) &= \frac{1}{2} \left(\frac{\Delta f_{peak}}{\sqrt{2} f_0} \right)^2 \left(\frac{f_0}{f_v} \right)^2 \\ &= \left(\frac{\bar{\Gamma} \bullet \bar{a}}{2 f_v} f_0 \right)^2. \end{aligned} \quad (5)$$

Or, when expressed in dB,

$$L(f_v) = 20 \log \left(\frac{\bar{\Gamma} \bullet \bar{a}}{2 f_v} f_0 \right). \quad (6)$$

Equation 6 may be rearranged to obtain

$$\Gamma_i = \frac{2 f_v}{a_i f_0} 10^{\left(\frac{L(f_v)}{20} \right)}, \quad (7)$$

where Γ_i is the component of acceleration sensitivity vector in the i ($i = x, y$ and z) direction. For a sinusoidal vibration, $|\bar{a}|$ is the peak applied vibration level in units of g , and $L(f_v)$ is expressed in units of dBc. In most cases, vibration experienced by an oscillator is random instead of sinusoidal. Under random vibration the power is randomly distributed over a range of frequencies, phases, and amplitudes, and the acceleration is represented by its power spectral density (PSD). For random vibration, $|\bar{a}| = \sqrt{2 PSD}$, and its unit is $g/\sqrt{\text{Hz}}$. Also, for a random vibration, $L(f_v)$ is expressed in units of dBc/Hz. The sum of acceleration

sensitivity squared in all three axes gives the total acceleration sensitivity, or gamma ($\bar{\Gamma}$), and its magnitude is defined as

$$|\bar{\Gamma}| = \sqrt{\Gamma_x^2 + \Gamma_y^2 + \Gamma_z^2}. \quad (8)$$

$\bar{\Gamma}$ of an oscillator can be calculated from equation 8 once the PM noise of the oscillator is measured for all three axes. Noteworthy to this discussion, the sidebands generated by oscillators under vibration are a more serious issue, as the signal frequency increases due either to frequency multiplication or direct frequency generation at higher frequency. Systems are in place that require ultralow PM noise from reference oscillators operating in the range of 6 to 18 GHz. The vibration-induced PM noise of an oscillator with frequency f_0 upon frequency multiplication by a factor of N is given by

$$L(f_v) = 20 \log \left[\frac{\bar{\Gamma} \cdot \bar{a}}{2f_v} (Nf_0) \right]. \quad (9)$$

The vibration frequency f_v is unaffected because it is an external influence. It is clear from equation 9 that, given a nominal $|\bar{\Gamma}| \sim 1 \times 10^{-9}/g$, the level of vibration sidebands in phase-noise plots of $L(f)$ can become excessively large at X-band and higher ranges. For example, a 10 MHz oscillator with a vibration sensitivity of $1 \times 10^{-9}/g$ when experiencing an acceleration of 5 g produces a sideband level of -72 dBc at $f_v = 100\text{Hz}$. For the same $|\bar{\Gamma}|$ and under identical vibration conditions, a 10 GHz oscillator will produce a sideband of -12 dBc, a factor of $20 \log(N=1000)$ higher. Often the sidebands are larger than the carrier, and there are also conditions where the carrier disappears and all of the power appears in the sidebands. This seriously affects or even prohibits the use of microwave systems that employ phase-locked loops, because large sidebands due to vibration cause large phase excursions and unlock the loops (Filler, 1988; Wallin et al., 2003).

3. Measurement Techniques

In order to measure the acceleration sensitivity of different microwave oscillators and components, the device needs to be characterized while subjected to vibration. The equipment needed to vibrate the device consists of a mechanical actuator or "shaker," its associated power amplifier, an accelerometer, and computer control system. The computer uses the accelerometer to sense the vibration of the actuator and generates the desired vibration profile using closed-loop feedback. The single axis actuator used for these tests has the capability to vibrate either in a random vibration pattern or in various sinusoidal patterns, including continuous wave and swept. When the actuator vibrates in one axis, the cross-axis leakage is low, as shown in Figure 3. These data are taken with a 3-axis accelerometer mounted on the actuator.

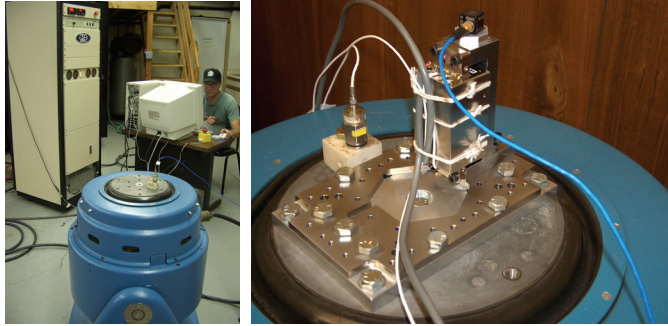


Figure 2. The picture on the left shows the vibration actuator (shown in blue); the amplifier for driving the actuator (the vertical rack-mount system); and the controlling computer. The picture on the right is a device under test (DUT) mounted on the actuator

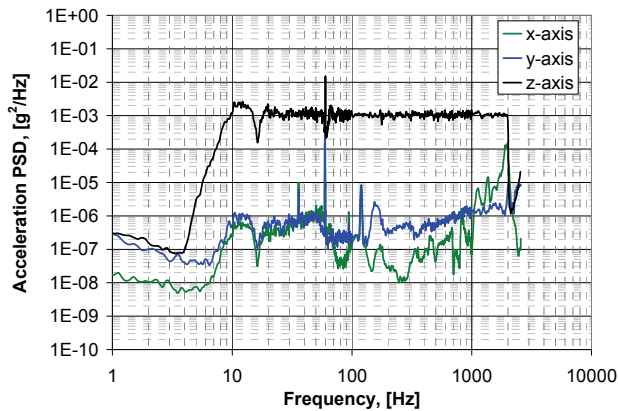


Figure 3. Plot showing the acceleration power spectral density (PSD) along x, y and z axes when vibration is along the z-axis, showing that cross-axis leakage is small. A random vibration profile of acceleration PSD = $1.0 \text{ mg}^2/\text{Hz}$ (rms) is used for $10 \text{ Hz} \leq f_v \leq 2000 \text{ Hz}$; f_v is the vibration frequency

For all the vibration tests discussed later, both sinusoidal and random vibration testing are chosen. First, a random vibration pattern is used, vibrating at frequencies between 10 and 2000 Hz, followed by a sinusoidal vibration at 10, 20, 30, 50, 70, 90, 100, 200, 300, 500, 700, 900, 1000, and 2000 Hz. This frequency range is chosen because it is the full range for the available vibration table, adequately covering smaller ranges associated with most applications (Section 5).

3.1 Experimental Setup for Residual PM Noise Measurement

Residual noise is the noise that is added to a signal by its passage through a two-port device. Figure 4 shows the block diagram of a PM noise measurement system used to measure the residual noise of a two-port or a non-oscillatory device such as a bandpass filter or amplifier as well as a cable and connector under vibration (Walls & Ferre-Pikal, 1999). The output power of a reference oscillator is split into two paths. One path is used to drive the device

under test (DUT), and the other path is connected to a delay line. The delay is chosen so that the delay introduced in one path is equal to the delay in the other path. A phase shifter is used to set phase quadrature or 90-degrees between two paths, and the resulting signals are fed to a double-balanced mixer, acting as a phase detector. The baseband signal at the output of the phase detector is amplified and measured on a fast Fourier transform (FFT) analyzer. The output voltage $V_0(t)$ is given by

$$V_0(t) = k_d G \Delta\phi(t) \quad \text{for } \Delta\phi(t) \ll 1, \quad (10)$$

where k_d is the mixer sensitivity, G is the gain of the baseband IF amplifier, and $\Delta\phi(t)$ is the difference in phase fluctuations between two inputs to the phase detector. The PM noise is obtained from

$$S_{\phi}(f) = \frac{PSD[V_0(t)]}{(k_d G)^2}. \quad (11)$$

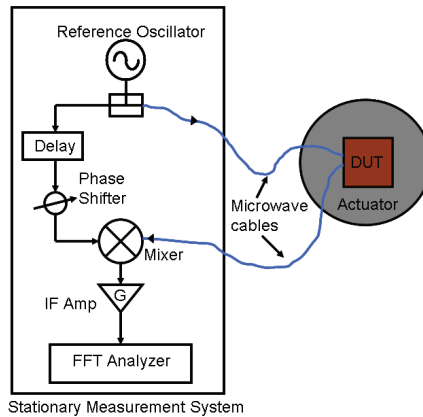


Figure 4. Block diagram of an experimental setup for residual PM noise measurement of components under vibration. DUT – Device Under Test; IF Amp – Intermediate Frequency Amplifier

Because the delays in the two signal paths are equal, the PM noise from the reference oscillator is equal and correlated in each path and thus cancels. At the output of the mixer, the noise from the vibrating DUT and connecting cables appears because it is not correlated between the two inputs of the mixer. A low noise phase detector and IF amplifier are chosen for this measurement and their noise contributions are much lower than the dominating vibration-induced noise of DUT and cables.

In order to accurately measure the vibration sensitivity of a DUT, it is very important to know the vibration sensitivity noise floor first. For the noise floor measurement, the DUT is replaced with an appropriate length of rigid coaxial cable. Compared to all other experimental components, it is the microwave cables, blue in color (Figure 4) and connected between the measurement system and the DUT mounted on the actuator that generally set the vibration sensitivity noise floor. When the DUT is under vibration, the cables flex

between the vibrating and stationary (measurement system) reference frames. The flexure of the cables causes the relative position between the different segments of the outer conductor, the dielectric, and the inner conductor of the cable to vary and thus changes the electrical characteristics of the cables. The main challenge is to obtain a reproducible low noise floor at close to carrier offset frequencies. The noise floor is very dependent on the configuration and tension of cables the running between the vibrating and stationary reference frames; a slight change may cause the noise to vary anywhere from 10 to 30 dB, as shown in Figure 5.

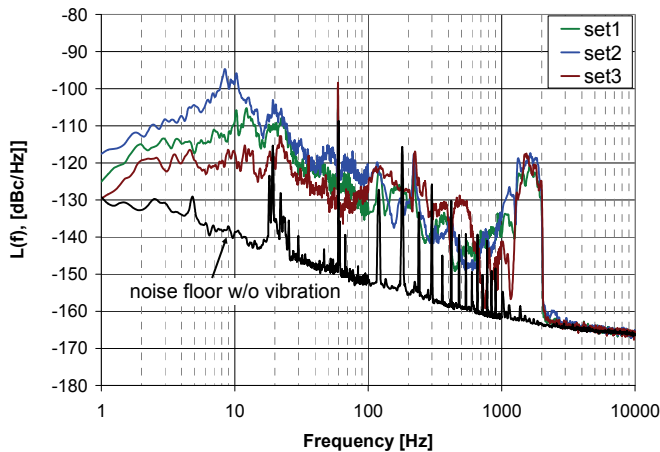


Figure 5. Residual PM noise floor of the measurement system measured with and without vibration. A random vibration profile of acceleration PSD = 1.0 mg²/Hz (rms) is used for 10 Hz ≤ f_v ≤ 2000 Hz. It shows the variation in the close to carrier noise for three different sets of measurement cable configurations. The bottom curve shows the noise floor measured under no vibration. Narrow spurs are power line EMI pick-up and should be ignored

Sometimes the noise floor is so high that it is impossible to accurately characterize low-vibration-sensitive components. In order to measure the acceleration sensitivity of a component accurately, the following precautionary measures should be taken:

- Rigidly mount the DUT on the vibration table to avoid any mechanical resonance inside the frequency range of interest.
- Experiment with different amount of cable slack or tension between the stationary and vibrating reference frames to obtain the best noise floor.
- Properly secure the cables to minimize flexing and strain due to vibration. It is also important to properly secure the power leads for the DUT.
- Reduce the acoustic noise and external vibration in the test area.
- The vibration actuator often has cooling fans; prevent this airflow from disturbing the cables.
- No other components except the DUT and accelerometer should be mounted on the vibration table.

- If possible, use 1 to 3 dB attenuators at the connector interfaces to minimize the effect of voltage-standing-wave-ratio (VSWR) induced mechanical and multipath phase fluctuations.
- Check the noise floor in between the measurements by replacing the DUT with a short cable.

3.2. Experimental Setup for Absolute PM Noise Measurement

Absolute noise is the noise measured on a one-port device such as an oscillator. Several measurement techniques can be used to measure the PM noise and thus the acceleration sensitivity of an oscillator. The most commonly used techniques are the heterodyne (two-oscillator) PM noise measurement system and the homodyne (delay-line discriminator) measurement system (Lance et al., 1984; Sullivan et al., 1990; Walls & Ferre-Pikal, 1999). In this section, these measurement techniques are briefly described. The block diagram of a single-channel heterodyne (two-oscillator) PM noise measurement system is shown in Figure 6. In this system, the signals from the DUT mounted on the vibration actuator and a stationary reference oscillator of the same frequency are fed into a double-balanced mixer. A lowpass filter (LPF) is used after the mixer to filter the higher-order harmonics, and a phase-locked loop (PLL) is used to lock the reference frequency to the DUT frequency and to maintain quadrature between the two input signals to the mixer. The output voltage of the mixer is proportional to the difference between the phase fluctuations of the two sources. This signal is amplified, and its power spectral density is measured on a FFT analyzer.

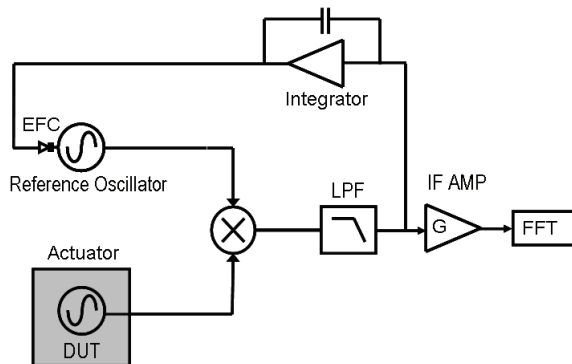


Figure 6. Block diagram for a heterodyne PM noise measurement system. DUT- Device Under Test; LPF – Low Pass Filter; EFC – Electrical Frequency Control; IF AMP – Intermediate Frequency Amplifier

The advantage of the heterodyne measurement system is its high sensitivity; however, there are notable disadvantages. It requires a reference oscillator of the same frequency, a PLL, and calibration of the mixer sensitivity (k_d). Among these, the main measurement uncertainty comes from the PLL. In order to measure the vibration induced PM noise at close to carrier offset frequencies, a low loop bandwidth is required. Furthermore, when the DUT experiences a large level of vibration, it may be difficult to keep the DUT and reference oscillator phase locked due to large phase excursions. This situation requires the PLL bandwidth to be increased, which complicates the calibration inside the PLL bandwidth.

A PM noise measurement system that needs neither a second source nor a phase-locked loop is a delay-line discriminator system, shown in Figure 7. As discussed in Section 3.1, in a residual PM noise measurement of a device, it is important to keep the delay in both signal paths as equal as possible so that the source noise is correlated and cancels at the phase detector. However, in a delay-line discriminator technique, introduction of a long delay in one path intentionally un-correlates the noise by increasing the delay time so that one can measure the PM noise of the source. The differential delay introduced in one path creates a frequency dependent phase shift between the two inputs of the phase detector. This frequency dependent phase shift converts frequency fluctuations of the source into differential phase fluctuations between the inputs of the phase detector. When these two signals are adjusted for phase quadrature, the phase detector converts the phase fluctuations into their voltage equivalent for measurement and analysis. The voltage at the output of the IF amplifier is given by

$$V_0(t) \cong (2\pi\nu_0 k_d \tau) G y_{rms}(t) = \nu_0 k_v G y_{rms}(t), \tag{12}$$

where ν_0 , τ , k_d , G , $y_{rms}(t)$, and k_v are respectively the carrier frequency, the time delay introduced by the delay line, the mixer sensitivity to phase fluctuations, the voltage gain of the baseband IF amplifier, the rms fractional frequency fluctuation and mixer sensitivity to frequency fluctuations. Equation 12 indicates that the output voltage of the mixer is proportional to the frequency fluctuation in the source; thus, this system measures the frequency modulated (FM) noise of the DUT. The FM and PM noises can be calculated from the following relations respectively,

$$\left. \begin{aligned} S_y(f) &= \frac{PSD[V_0(t)]}{(\nu_0 k_v G)^2} \\ S_\phi(f) &= \left(\frac{1}{f^2}\right)^2 \frac{PSD[V_0(t)]}{(k_v G)^2} \end{aligned} \right\} \text{for } f \ll 1/\tau. \tag{13}$$

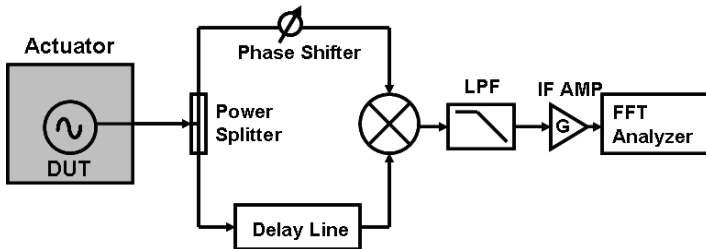


Figure 7. Block diagram of a measurement system that uses a delay-line to measure PM noise of an oscillator under vibration

The close to carrier noise floor of a delay line discriminator measurement is inversely proportional to the time delay, τ . By increasing the time delay, the noise floor can be lowered; however, longer delay causes higher insertion loss of the RF signal thus reducing

measurement sensitivity, which effectively increases the noise floor. This problem can be overcome by use of a low loss delay, such as a photonic delay line (Rubiola et al., 2005). The long fiber delay provides a low-loss carrier of RF signals. A 2 km fiber typically provides 0.4 dB loss and about 10 μ s delay whereas insertion loss due to a 25 m semi-rigid cable at 10 GHz is approximately 20 dB with a delay of about 100 ns. Using a 10 μ s photonic delay instead of a 100 ns RF delay, almost 40 dB of improvement in the noise floor can be achieved.

There is another technique known as direct digital PM noise measurement (Grove et al., 2004), which requires two sources similar to a heterodyne technique. However, like a delay line discriminator technique it needs no phase-locked loop. This PM noise measurement system uses fast analog-to-digital converters to digitize the input RF signal and performs all down-conversion and phase detection functions by digital signal processing. It provides a low noise floor, require no calibration of k_d or k_v , and can compare oscillators at different frequencies. High dynamic range with no phase-locked loop involved means the PM noise of a vibrating noisy source can be measured accurately for offset frequencies very close to the carrier. Figure 8 shows the setup used to measure acceleration sensitivity of different microwave oscillators discussed in Section 5.2 using this measurement system. The oscillator under test is mounted on a vibration table with the output going to one input of a mixer. This output is then mixed with a very-low-PM-noise oscillator to generate a beat frequency anywhere between 1 MHz to 30 MHz for the most straightforward digitizers. A low-noise 10 MHz quartz crystal oscillator serves nicely as the digitizer's reference clock.

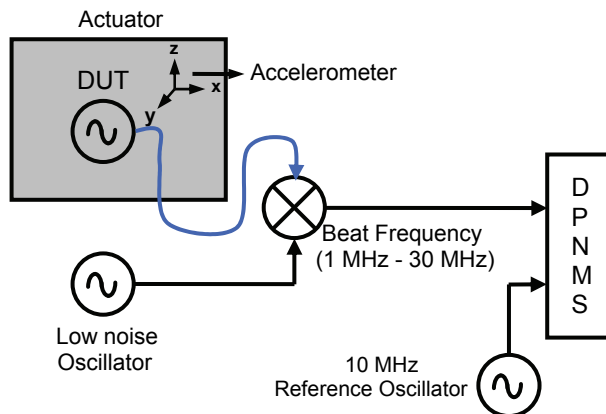


Figure 8. Block diagram of an experimental setup for measuring acceleration sensitivity of an oscillator. DPNMS – Direct digital PM noise measurement system

4. Results - Acceleration Sensitivity of Non-oscillatory Devices

Most microwave components are sensitive to vibrations to some extent. Among them, microwave cables, bandpass filters, mechanical phase shifters and connectors are the most sensitive. Therefore, it is very important to select vibration-tolerant components in order to build a system with low vibration sensitivity. The local oscillator is one of the prime

performance-limiting components in an RF receiver. However, with increasing demand for low acceleration sensitivity of oscillators in various applications, the sensitivity to vibration of these non-oscillatory components will soon be the limiting factor and thus cannot be ignored (Driscoll & Donovan, 2007). In this section, the performance of some of the non-oscillatory microwave and optical components under vibration is discussed. The components used for test are commercially available and shown in Figure 9.

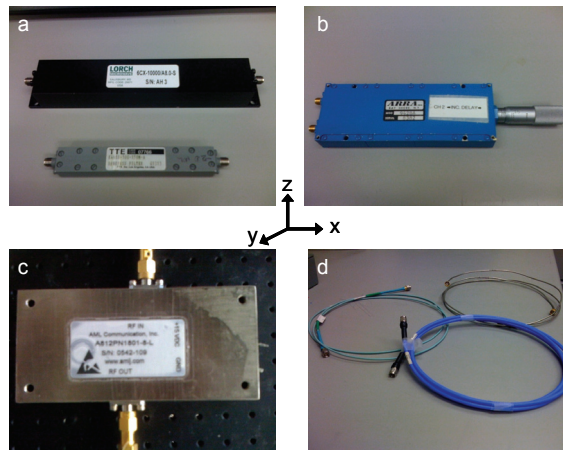


Figure 9. Picture of the non-oscillatory components used for vibration test. (a) Bandpass filter, (b) Mechanical phase shifter, (c) Amplifier and (d) Microwave cables. Arbitrary x and y axes are chosen in the plane of the page, and the z-axis is normal to the page

4.1 Microwave Components

First, two 10 GHz bandpass cavity filters of different quality factors (Q) are tested under random vibration. A random vibration profile of acceleration PSD $1.0 \text{ mg}^2/\text{Hz}$ (rms) for offset frequencies 10 Hz to 2000 Hz is used. Figure 10(a) shows the PM noise floor of the measurement system as well as the PM noise of the filters under vibration. A comparison of acceleration sensitivity of these filters in rad/g is shown in Figure 10(b). The result is obtained by converting $L(f)$ to $S_{\phi}(f)$ using equation 4 and dividing it by $|\vec{a}| = \sqrt{2PSD}$. The result shows that the filter with higher Q (narrow bandwidth) is more sensitive to vibration. This is due to the fact that the transfer function phase of a band pass filter has its steepest slope at the center frequency. Any vibration that modulates the resonant structure of the filter also modulates the center frequency and thus the phase shift through the filter. The phase slope is proportional to the filter Q ; this causes the high- Q filter to be more sensitive to small mechanical distortions under vibration. Figure 10(b) also indicates that the microwave cables used for the measurement set a noise floor that provides an acceleration sensitivity of 10^{-4} to $10^{-6} \text{ rad}/g$. For perspective, this means that in order to measure a 10 GHz oscillator with an acceleration sensitivity of $10^{-12}/g$ experiencing a random noise of $0.05 \text{ g}^2/\text{Hz}$ (rms) between $10 \text{ Hz} \leq f_v \leq 1000 \text{ Hz}$, the cable should have vibration sensitivity better than $7 \times 10^{-4} \text{ rad}/g$ and 7×10^{-6} at offset frequencies 10 Hz and 1000 Hz, respectively.

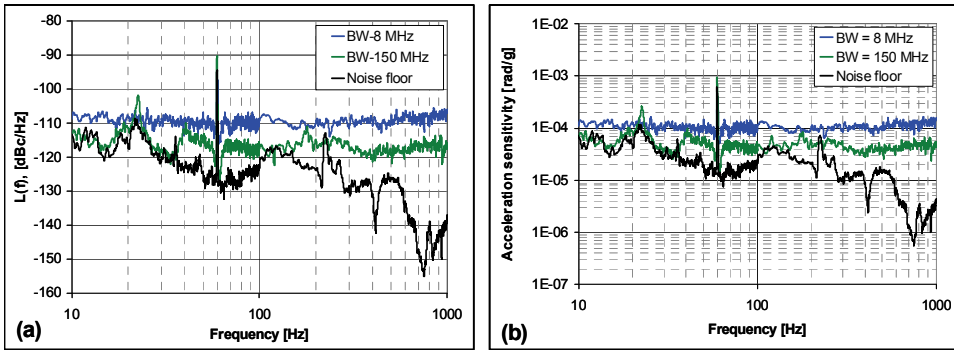


Figure 10. (a) PM noise of two 10 GHz bandpass cavity filters under vibration. A random vibration profile of acceleration PSD = 1.0 mg²/Hz (rms) is used for 10 Hz ≤ f_v ≤ 2000 Hz. The bottom curve shows the PM noise floor set by flexing of cables under vibration. (b) Acceleration sensitivity of the same two 10 GHz bandpass cavity filters. BW is the bandwidth of band pass filter

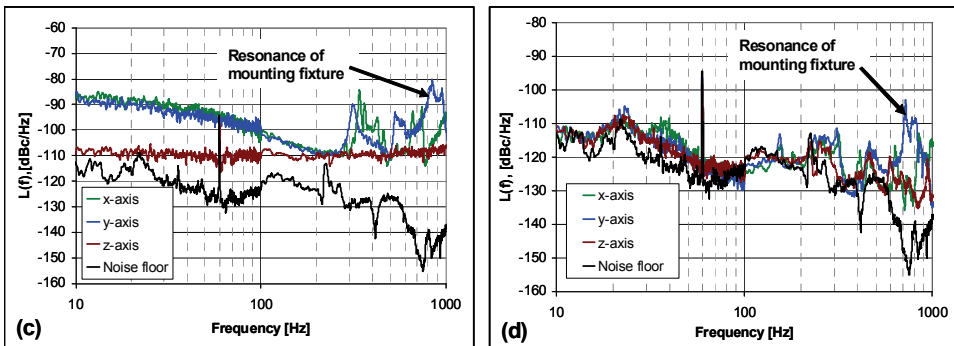


Figure 10. (c) PM noise of a 10 GHz high-Q band pass filter along x, y and z axes. (d) PM noise of a mechanical phase shifter along x, y and z axes. A random vibration profile of acceleration PSD = 1.0 mg²/Hz (rms) is used for 10 Hz ≤ f_v ≤ 2000 Hz

The PM noise of a high-Q bandpass filter and a mechanical phase shifter is measured along all three axes. See Figure 9 for the orientation of the axes. Figure 10(c) shows the PM noise of a bandpass filter under vibration along all three axes. Close to the carrier, the filter is more sensitive to vibration along the x- and y-axis than along the z-axis. It is also important to note that sometimes the mechanical resonances of the fixture used to mount the component on the actuator can appear. This effect is visible for the bandpass filter above 300 Hz. Therefore, it is important to either minimize this effect, if possible, or separate it from the results of actual vibration induced noise. In the case of the phase shifter, the noise is limited mostly by the noise floor of the measurement system, as shown in Figure 10(d).

Next, three different types of cables, viz. flexible, hand formable and semi-rigid cables, each 12 feet long, are chosen for the noise floor measurement. The PM noise floors set by each of these cables under vibration are comparable, similar to that shown in Figure 5. Finally, the PM noises of a few amplifiers at 10 GHz are also measured under vibration (Hati et al. 2007). The acceleration sensitivity of these components is much lower than the acceleration

sensitivity noise floor provided by the cables. As a result, an accurate measurement is not possible. However, it can be concluded from the experimental results that the acceleration sensitivity of the phase shifter and amplifier under test is no greater than 10^{-4} rad/g.

4.2 Optical Components

Optical fibers are widely used in fiber-optic communication, ring-laser gyroscopes, optoelectronic oscillators (OEOs), and delay line discriminators, among a number of other applications (Yao & Maleki, 1996; Römisch et al., 2000; Kadiwar & Giles, 1989; Rubiola et al., 2005; Minacian, 2006). Mechanical distortions due to vibration induce phase fluctuations in the fiber. In this section, the effect of vibration on the phase fluctuations in the optical fiber wound on a spool is discussed. Letting l be the length of the fiber (assumed to be uniformly wound on a cylindrical spool) and v_g the group velocity of amplitude modulated electromagnetic waves down the fiber; then the group delay through the fiber is $\tau_d = l/v_g$. In fiber, stretching can occur either as a result of temperature changes of the spool on which the fiber is wound or as a result of axial vibrations that accelerate, and hence, deform the spool. The fiber length change (δl) due to deformation of spool, which is mounted at the bottom, is given by (Ashby et al., 2007)

$$\frac{\delta l}{l} = \frac{\nu \rho a(t) h}{2E}, \quad (14)$$

where ν , ρ , $a(t)$, h and E are, respectively, Poisson's ratio of the spool material, spool density, time-dependent acceleration, height of the spool, and Young's modulus (describing the spool's stiffness). Equation 14 shows that the stiffer the spool, the smaller the length change, and the denser the spool, the larger the length change, because the force on the fiber is larger. It also shows a linear dependence on the time-dependent acceleration. Further, a change in length due to stretching will also result in stresses within the fiber that can change the optical properties of the fiber, resulting in a change in the group velocity through its stress-optic coefficients. When these changes are small, the fractional frequency shift is a superposition of these two contributions:

$$\frac{\delta f}{f_0} \approx \frac{1}{v_g} \left(\frac{\delta v_g}{\delta \left(\frac{\delta l}{l} \right)} - v_g \right) \frac{\delta l}{l}. \quad (15)$$

The changes in the group velocity for a stretched fiber are quite small, and we can neglect them in a first approximation so that the fractional frequency shift due to vibration-induced fiber length changes can be adequately approximated by

$$\frac{\delta f}{f_0} \approx -\frac{\delta l}{l}. \quad (16)$$

Thus, when used in an optoelectronic oscillator, which is described in Section 5.2, the main effect on a desired frequency comes from the change of length itself rather than from the change in group velocity. The small time-delay fluctuations due to fiber length fluctuations

inside the loop directly map to larger frequency fluctuations at the output of the oscillator (Leeson, 1966), which is principally why suppressing fiber vibration sensitivity is so important.

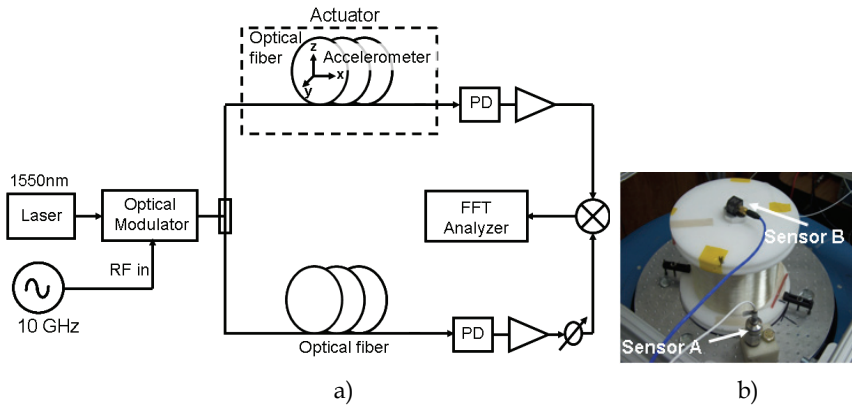


Figure 11. (a) Experimental setup to study vibration-induced PM noise in a fiber delay line mounted on a vibration table. (b) Optical fiber of length 3 km wound on a ceramic spool and mounted on a vibration table. Orientation as shown presents the vibration (acceleration) along the z-axis of spool

Figure 11(a) shows the setup used to measure the effect of vibration on a fiber delay line using a residual PM noise measurement. It consists of a 1550 nm communications-grade laser whose output is sent into an optical modulator that is amplitude-modulated by a 10 GHz RF signal. This RF-modulated optical signal is then split into two signal paths, each composed of a 3 km length of single mode fiber (SMF-28) wound on a cylindrical spool, a photo-detector, an RF amplifier, and a phase shifter. As discussed earlier, a mechanical phase shifter is used to set phase quadrature between the two signals so that the output voltage noise of the mixer is proportional to the PM noise. This signal is then measured on a FFT analyzer. Because the delays in the two signal paths are equal, this technique cancels the PM noise introduced by the laser, optical modulator, and the reference oscillator.

In order to test the vibration properties of the fiber, one of the 3 km fibers wound on a stiff cylindrical ceramic spool is secured to a vibration table. The cylindrical spool is approximately 11.5 cm in diameter with a length between end caps of 10 cm. An accelerometer mounted to the actuator, as shown in Figure 11(b) (sensor A), provides closed-loop feedback to a computer for control of the vibration profile. Sensor B is a triaxial accelerometer that is used to sense vibrations affecting the fiber spool. Its z-axis is aligned with the axis of the spool, and both the x and y axes are in the radial directions. For this test, the z-axis sensitivity is the subject of consideration because the vibration sensitivity of a fiber-on-spool is greatest along this axis (Ashby et al. 2007; Huang et al. 2000). The spool is subjected to a random vibration of acceleration PSD equal to $0.5 \text{ mg}^2/\text{Hz}$ (rms) along the z-axis, and the PM noise is measured. In Figure 12, the bottom curve is the noise floor, and the topmost curve is the same measurement of PM noise under vibration. The dotted brown line shows that the acceleration sensitivity of this fiber is $2.5 \times 10^{-3} \text{ rad/g}$, which is calculated for $L(f) = -85 \text{ dBc/Hz}$. The resonance at 600 Hz is a characteristic of the hollow cylindrical spool geometry. The ceramic spool is chosen due to its stiffness because it is less sensitive to

vibration than other materials such as plastics (Taylor et al., 2008). The measurement of acceleration sensitivity of other optical components such as optical connectors, fiber laser, optical modulator, and photo-detector are also important; however, the largest sensitivity to vibration is usually from the fiber.

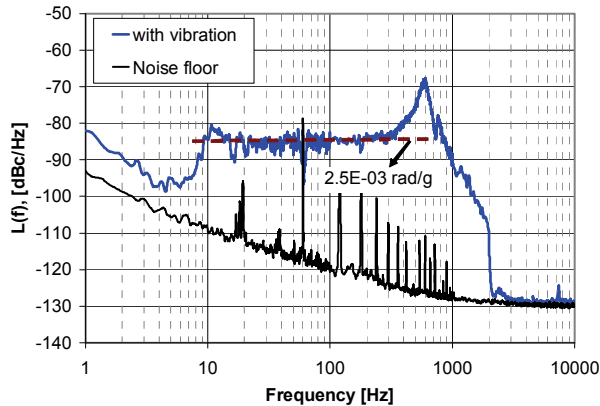


Figure 12. The residual PM noise of a 3 km fiber under random vibration along the z-axis is shown. A random vibration profile of acceleration PSD of $0.5 \text{ mg}^2/\text{Hz}$ (rms) is used for $10 \text{ Hz} \leq f_v \leq 2000 \text{ Hz}$. The dotted brown curve shows the acceleration sensitivity corresponding to $L(f) = -85 \text{ dBc/Hz}$. The bottom curve is the noise floor measured under no vibration

5. Results - Acceleration Sensitivity of Different Classes of Oscillators

Low-noise oscillators must operate under “real world” vibration/acceleration conditions. This is crucial for high-speed communications systems, advanced surveillance systems, weapons detection, and many other applications. The PM noise requirement for each application is different, and a single oscillator cannot meet the PM noise requirement over a broad range of offset frequencies. For example, a good low noise 10 MHz quartz oscillator typically has a PM noise $L(10 \text{ Hz}) = -130 \text{ dBc/Hz}$ and a white PM noise level of -170 dBc/Hz . The PM noise of this 10 MHz signal at 10 Hz offset, when multiplied to generate a signal at 10 GHz, becomes -70 dBc/Hz , which is reasonably low and suitable for a 10 GHz radar to detect slow-moving objects (Fruehauf, 2007). However, the white PM noise after ideal multiplication becomes -110 dBc/Hz and is too high to detect fast-moving targets such as supersonic aircraft. There are several X-band oscillator topologies such as a YIG (Yttrium, Iron and Garnet) oscillator, dielectric resonator oscillator (DRO), surface transverse wave (STW) oscillator, sapphire loaded cavity oscillator, or a simple air-dielectric cavity resonator oscillator that can provide very low phase noise at higher offset frequencies. A combination of any of these oscillators with a quartz oscillator can achieve a low PM noise performance over a broad frequency range.

Oscillators that are capable of satisfying specific system requirements in quiet environments are readily available. However, in the vibrating environments of airborne platforms, the PM noise of oscillators degrades significantly. Table 1 and Figure 13 show the typical level of acceleration for certain operating environments (Mancini, 2004). Acceleration levels at the

oscillator depend on how and where the oscillator is mounted. Platform resonances can greatly amplify the acceleration levels.

Environment	Acceleration typical levels, in units of g
Tractor-trailer (3-80 Hz)	0.2 peak
Armored personnel carrier	0.5 to 3 rms
Ship – calm seas	0.02 to 0.1 peak
Ship – rough seas	0.8 peak
Propeller aircraft	0.3 to 5 rms
Helicopter*	0.1 to 7 rms
Missile – boost phase	15 peak
Jet aircraft*	0.02 to 2 rms

Table 1. Typical level of acceleration for certain operating environments. * See Figure 13

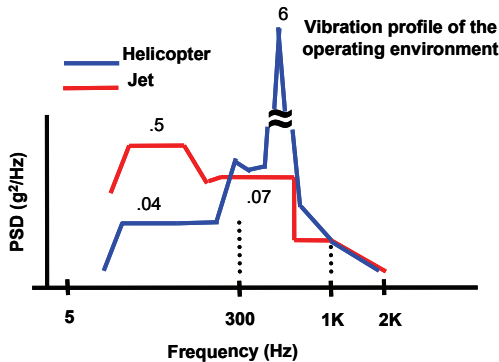


Figure 13. Typical aircraft random vibration profile

Section 5 is primarily focused on studying the effect of vibration on the phase noise of electronic and opto-electronic oscillators at 10 GHz and also comparing their acceleration sensitivity. The acceleration sensitivity of a quartz oscillator is not discussed here because enormous amounts of work have already been done and the data are readily available in the literature (Vig, 1992; Driscoll, 1993; Filler, 1983; Kosinski, 2000). A good quartz oscillator typically has an acceleration sensitivity of $1 \times 10^{-9}/g$, and the lowest known acceleration sensitivity for a quartz oscillator is $2 \times 10^{-11}/g$ for $10 \text{ Hz} \leq f_v \leq 200 \text{ Hz}$ (Bloch et al., 2006).

5.1 Electronic Oscillators

Figure 14 shows three different types of oscillators chosen for the vibration test, viz., a DRO at 10 GHz, a silicon germanium (SiGe) amplifier-based STW oscillator at 2.5 GHz (Hay, et al., 2004), and a TE_{023} mode air-dielectric ceramic-cavity resonator oscillator (ACCRO) at 10 GHz (Hati et al., 2006). A STW oscillator is chosen because these are the best performing oscillators in the frequency range 1 to 3 GHz. Below 1 GHz surface acoustic wave (SAW) oscillators perform well (Parker & Montress, 1988), and above 3 GHz DROs provide the best

compromise between performance and cost. There are several other commercially available oscillators above 3 GHz that have extremely low phase noise but are large, specialized and expensive by comparison. At first, the PM noise of these oscillators is measured with no vibration; the PM noise plots are shown in Figure 15.

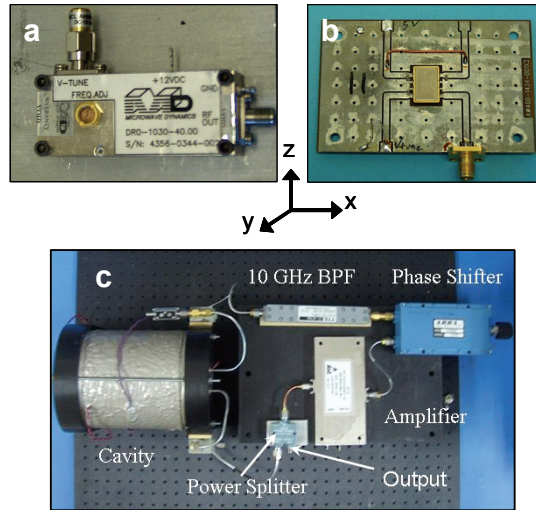


Figure 14. Pictures of three different types of oscillators used for vibration test. (a) DRO, (b) STW oscillator, (c) ACCRO. Arbitrary x and y axes are chosen in the plane of the page, and the z-axis is normal to the page

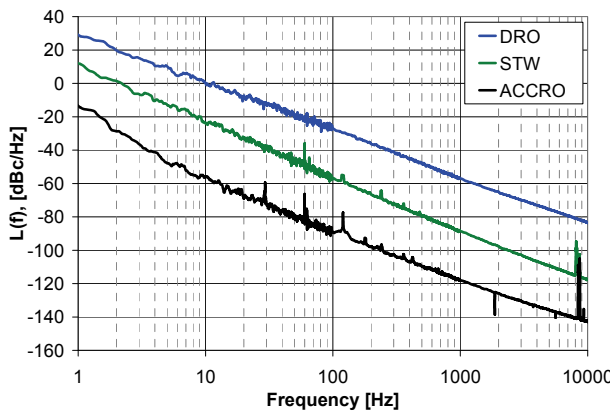


Figure 15. PM noise of three different oscillators at 10 GHz without vibration. For straight comparison, the PM noise of 2.5 GHz STW oscillator is normalized to 10 GHz

A commercial DRO at 10 GHz is subjected to a random vibration along three axes independently. The degradation in PM noise due to vibration in the z-axis is shown in Figure 16(a). The effect of random vibration in the x and y axes is not noticeable because the PM noise of the stationary DRO is much higher than the noise induced by random vibration.

In order to measure the acceleration sensitivity in all three axes, the oscillator is subjected to sinusoidal vibration with higher g-levels at different frequencies. The results are shown in Figure 16(b). This particular DRO is more sensitive to vibration along the z-axis than along the other two axes. Further, the acceleration sensitivities of two DROs of comparable size and weight but different Q are compared. Figure 17(a) and 17(b) respectively show the PM noise and acceleration sensitivity of these DROs. The DRO with higher Q is more sensitive to vibration for the same reason as discussed in Section 4.1 for a high-Q bandpass filter.

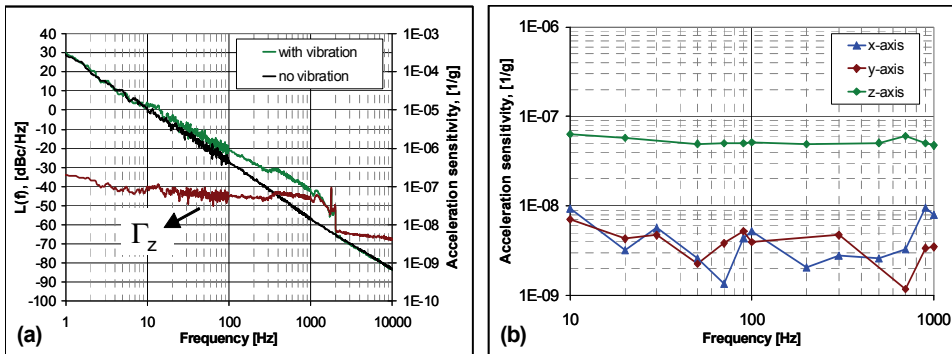


Figure 16. (a) PM noise of the DRO with and without vibration along the z-axis. The brown curve indicates the z-axis acceleration sensitivity of this particular DRO. (b) x, y, and z-axis gamma. An acceleration PSD of $0.5 \text{ mg}^2/\text{Hz}$ (rms) is used for random vibration (Fig. 16a) and a peak acceleration of 1 g is used for sinusoidal vibration (Fig. 16b)

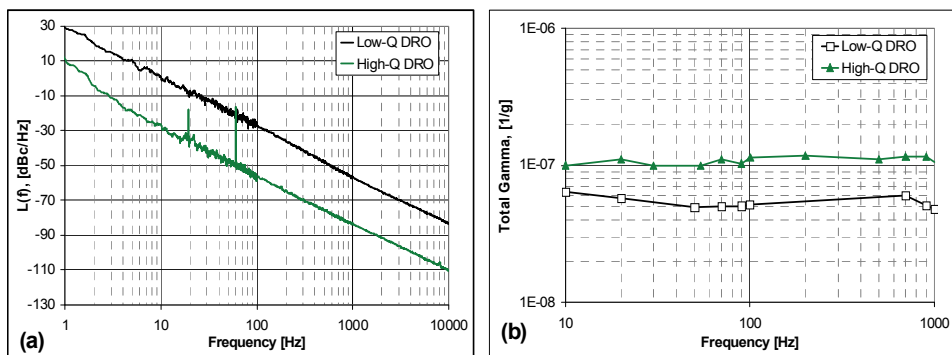


Figure 17. (a) PM noise of two DROs of different Q without vibration. (b) Plot of total gamma for the DROs. An acceleration PSD = $0.5 \text{ mg}^2/\text{Hz}$ (rms) is used for $10 \text{ Hz} \leq f_v \leq 2000 \text{ Hz}$. The lower PM noise oscillator has correspondingly higher acceleration sensitivity

Vibration-sensitivity experiments are also performed for a STW oscillator in all three axes, and the results are shown in Figure 17(c). For the ACCRO, the vibration measurement is confined to a single axis normal to the mounting plate, as shown in Figure 10. Figure 17(d) shows the z-axis acceleration sensitivity of three oscillators; the acceleration sensitivity of the STW oscillator is two orders of magnitude lower than that of the DRO.

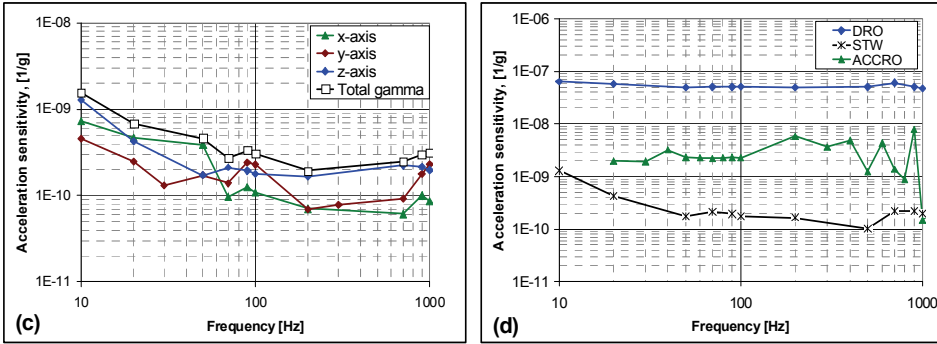


Figure 17. (c) x, y and z-axis acceleration sensitivity of a STW oscillator. (d) Comparison of z-axis acceleration sensitivity of different oscillators. A peak acceleration of 1 g is used

5.2 Optoelectronic Oscillator

Low-noise, microwave-frequency oscillators are key components of systems that require high spectral purity. An optoelectronic oscillator (OEO) is an example that has emerged as a low-noise source in recent years (Yao & Maleki, 1996; Römisch et al., 2000; Eliyahu et al., 2008). The high spectral purity signal of an OEO is achieved by using a long optical fiber that provides a very high quality factor (Q). However, the close to carrier spectral purity of an OEO is degraded mostly by environmental sensitivities, one being the vibration-induced phase fluctuations in its optical fiber (Howe et al., 2007; Hati et al., 2008).

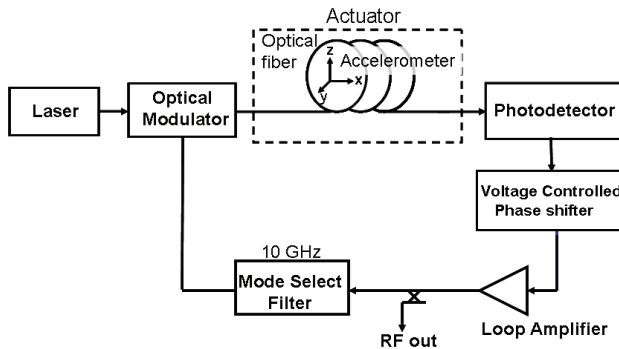


Figure 18. Block diagram of an optoelectronic oscillator

In a typical optoelectronic device as shown in Figure 18, light from a laser passes through an electro-optic amplitude modulator, the output of which is fed to a long optical fiber and detected with a photodetector. The output of the photodetector is then amplified, filtered, and fed back to the modulator port, which amplitude-modulates the laser light. When loop gain is greater than 1, this configuration leads to self-sustained oscillations. A typical OEO gives a large number of modes with frequencies given by (Yao & Maleki, 1996; Römisch et al., 2000)

$$f_0 = \frac{(K + 1/2)}{\tau_d} \tag{17}$$

where K is an integer whose value is selected by the filter and $\tau_d = l/v_g = nl/c$ is the group delay through the fiber with index of refraction n and length l and c is the velocity of light. The quality factor of an OEO is proportional to length l and is given by $Q = \pi\tau_d f_0 = \pi n l f_0 / c$. An OEO at 10 GHz is designed by using the same 3 km (SMF-28) fiber as mentioned in Section 4.2 to study the effect of vibration on the overall PM noise performance of the oscillator. The PM noise of this OEO subjected to random vibration is shown in Figure 19. The PM noise under vibration degrades almost 30 to 40 dB from its normal stationary PM noise performance. This is due to the fact that the phase perturbations due to vibration in the fiber, which is the most vibration sensitive component in the loop, translate to frequency fluctuations inside the OEO’s resonator bandwidth. The z-axis acceleration sensitivity of this OEO is approximately $5 \times 10^{-9}/g$, as shown by the brown plot in Figure 19.

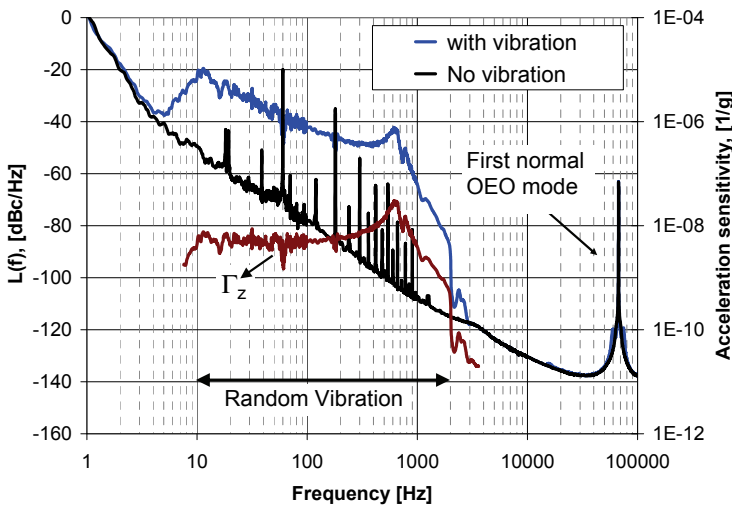


Figure 19. Plot comparing the PM noise of an optoelectronic oscillator with and without vibration. A random vibration profile of acceleration PSD = 0.5 mg²/Hz (rms) is used for 10 Hz ≤ f_0 ≤ 2000 Hz. The brown curve shows the z-axis acceleration sensitivity of this OEO, which is approximately $5 \times 10^{-9}/g$. The first mode for a 3 km fiber, which is approximately 67 kHz from the carrier, is also shown

6. Acceleration Sensitivity Reduction

In this section, a few methods of reducing vibration-induced noise from vibration-sensitive components are discussed. The most common approach for reducing vibration-induced PM noise is to select low-vibration-sensitive materials. A comparison is made for two air-dielectric cavity oscillators at 10 GHz, one cavity made of aluminum and another one made of ceramic. The two cavities are chosen so that they have comparable volume, almost identical loaded Q 's of 22,000 (TE₀₂₃ mode) and insertion losses of 6 dB. All the other

components of the two oscillators are identical. These two oscillators are tested for different sinusoidal vibration frequencies. The acceleration sensitivity of the ceramic cavity oscillator is found to be almost one sixth that of the aluminum cavity oscillator, as shown in Figure 20. This is because ceramic is stiffer than aluminum and thus less sensitive to vibration.

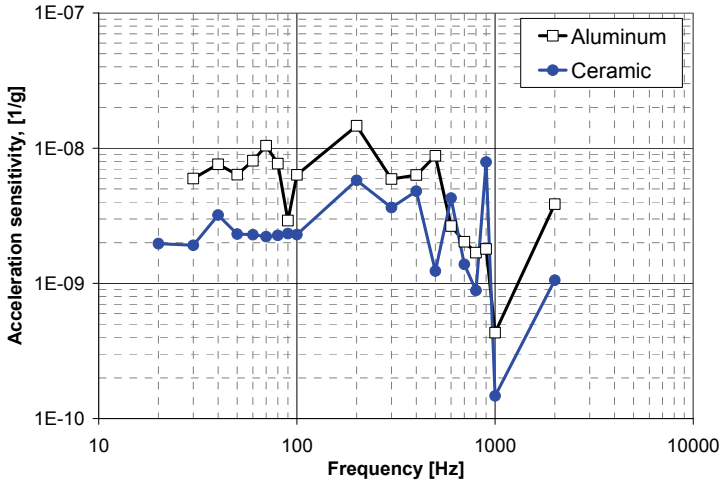


Figure 20. Comparison of acceleration sensitivity of aluminum and ceramic air-dielectric cavity resonator oscillators

It is also worth noting the results of a few tests of passive mechanical dampers and isolators on different test oscillators. The most common approach to reduce vibration-induced PM noise is to select vibration isolators of low natural frequency. Small stranded wire rope isolators and urethane shock mounts, as shown in Figure 21(a), provide excellent damping and omnidirectional isolation. When size is critical, these small shock absorbers are often incorporated inside the oscillator package to improve the PM noise performance of the oscillator in high vibration induced environments. Further, when space is not an issue, an external vibration isolation platform can be used. In this case, the whole system including the oscillator can be mounted on this vibration-free platform to achieve the precision needed for the particular application. There are several commercially available vibration isolation platforms with extremely good performance and very low natural resonance frequencies, less than 1 Hz. A significant improvement in the acceleration sensitivity of the DRO and STW oscillators is observed when tested under vibration with these passive dampers as shown in Figure 21(b).

Finally, an active electronic vibration cancellation technique can be sometimes used to reduce the vibration sensitivity. A 3 km long optical fiber and an optoelectronic oscillator are chosen to illustrate this scheme. Work on control of environmental noise in optical fiber has previously been implemented in systems where either a portion of the system undergoes vibration or a stable reference is available to measure the vibration-induced noise (Foreman et al., 2007). It is very important to assess the degree to which vibration induced phase fluctuations $\phi_v(t)$ can be correlated with and predicted by an accelerometer so that it becomes possible to electronically cancel the effect of vibration-induced noise in the fiber (Hati et al., 2008).

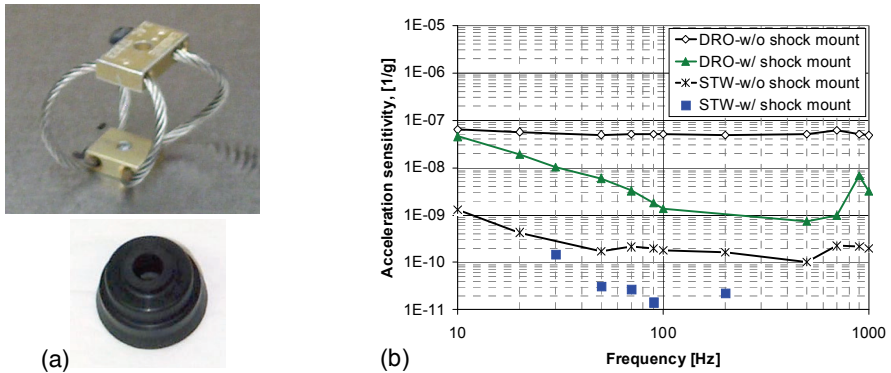


Figure 21. (a) Wire-rope and urethane passive shock mounts. (b) Improvement in acceleration sensitivity resulting from use of shock mounts

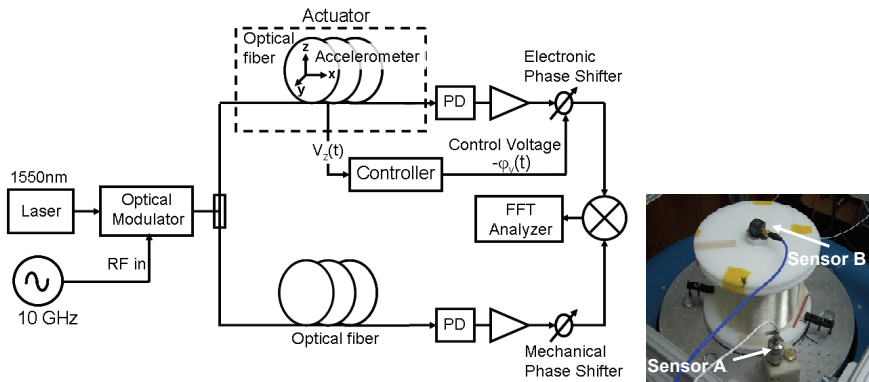


Figure 22. Experimental setup to study vibration-induced PM noise and its suppression in a fiber delay line mounted on a vibration table. PD is a photodetector that converts 10 GHz optical modulation to RF

The 3 km optical fiber (SMF-28) wound on a ceramic spool is subjected to vibration. While the fiber is under vibration, an estimate of the opposite phase of the $\phi_o(t)$ signal is generated based on vibration sensors, in this case, a z-axis accelerometer (sensor B) mounted on the top of the spool. The z-axis is the most sensitive axis, by an order of magnitude or more compared to the x and y axes (Ashby et al. 2007, Huang et al. 2000). An electronic phase shifter, as shown in Figure 22, corrects the phase perturbations of the demodulated 10 GHz signal sensed by the accelerometer by feed-forward correction. Figure 23(a) shows preliminary results and proof-of-concept of active noise control applied to the ceramic spool of optical fiber. The bottom curve is the noise floor, and the topmost curve is the same measurement of PM noise while the spool is subjected to a random vibration. The middle curve is the residual PM noise with the noise control on. Particularly noteworthy is that the residual PM noise through the spool of fiber is reduced by 15 dB to 25 dB. For this experiment, a flat frequency response is used for the feed-forward phase correction. The acceleration sensitivity of 3 km fiber with and without feed-forward cancellation is also shown in Figure 23(b).

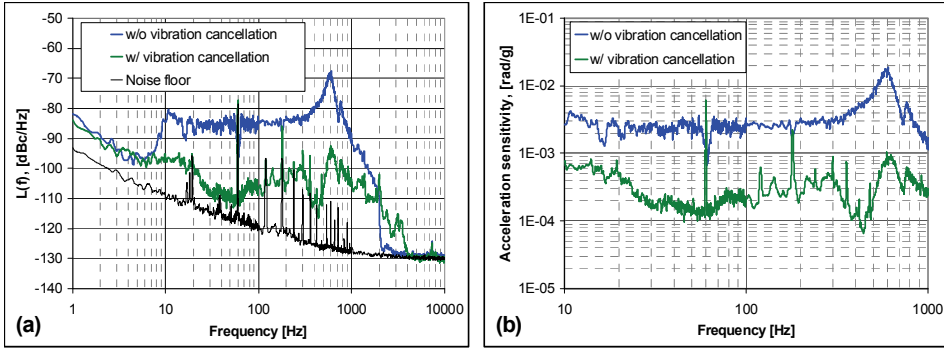


Figure 23. (a) Plot comparing the residual PM noise of fiber under random vibration with and without feed-forward cancellation. (b) Acceleration sensitivity of a 3 km fiber with and without feed-forward cancellation. A random vibration profile of acceleration PSD = 0.5 mg²/Hz (rms) is used for 10 Hz ≤ f_v ≤ 2000 Hz

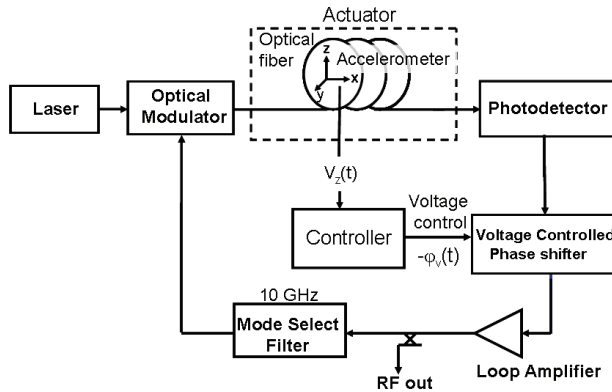


Figure 24. Block diagram of an OEO with active vibration-induced noise control

The same technique is implemented in an OEO to cancel the vibration-induced noise. In an OEO under vibration, an accelerometer signal is used to accurately estimate the complex conjugate of the vibration-induced phase modulation, as depicted in Figure 24. This estimate modulates the oscillator’s output frequency by virtue of Leeson’s model (Leeson, 1966) in such a way as to correct the induced in-loop phase perturbations. The PM noise of the 10 GHz OEO with and without vibration, as well as with vibration cancellation, is shown in Figure 25(a). Finally, the z-axis acceleration sensitivity of the OEO at 10 GHz is calculated by use of equation 7 and Figure 25(a) and is shown in Figure 25(b). There is an improvement by almost an order of magnitude in acceleration sensitivity over the full range of vibration frequencies tested. A flat frequency response is used for the feed-forward phase correction in this case. However, a custom-tailored frequency response can be used to achieve better cancellation at different vibration frequencies. In order to verify this, the fiber spool is subjected to a sinusoidal acceleration of 1 g at 10 Hz, 50 Hz, 100 Hz, 200 Hz and 1 kHz. The bottom curve of Figure 25(b) shows that further improvement in z-axis sensitivity is

achieved by optimizing the phase and amplitude of the feed-forward phase correction at these specific sinusoidal frequencies.

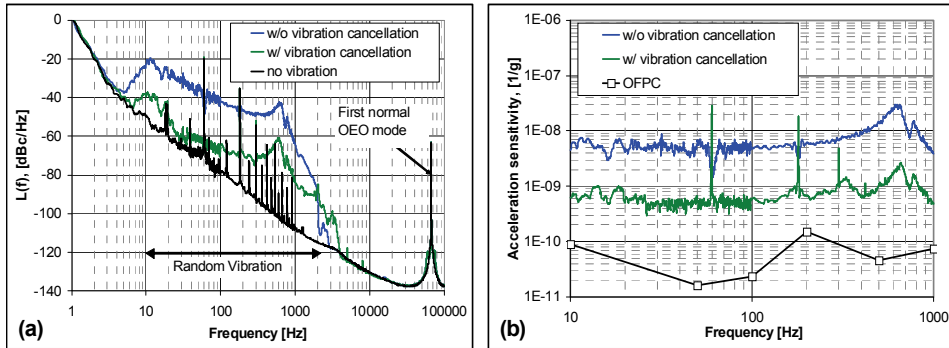


Figure 25. (a) PM noise of a 10 GHz OEO with and without vibration cancellation. A random vibration profile of acceleration PSD of $0.5 \text{ mg}^2/\text{Hz}$ (rms) is used for $10 \text{ Hz} \leq f_v \leq 2000 \text{ Hz}$. (b) Plot of z-axis acceleration sensitivity with and without vibration cancellation. The bottom curve corresponds to a single-frequency sinusoidal peak acceleration of 1 g. For each sinusoidal frequency, an optimized feed-forward phase correction (OFPC) is used

7. Conclusion

Structure-borne vibration is routine for many applications, causing an increase in PM noise of oscillators that disables many systems. Therefore, it is very important to select components that show low phase changes under vibration in order to build a system with low vibration sensitivity. In this chapter, the acceleration sensitivity and its relation to PM noise of an oscillator is derived. Different techniques for measuring the PM noise level of components under vibration are also discussed. The acceleration sensitivity of several state-of-the-art microwave and optical components are measured. Results show that high-Q components are generally more sensitive to vibration. Finally, different passive and active techniques to suppress or cancel vibration-induced noise in these oscillators are also discussed. Results show that proper use of passive and active cancellation schemes can improve the acceleration sensitivity of an oscillator by several orders of magnitude.

8. Acknowledgement

The authors thank Neil Ashby, Jeff Jargon and Jennifer Taylor for useful discussion and valuable suggestions.

9. References

- Ashby, N.; Howe, D. A.; Taylor, J.; Hati, A. & Nelson, C. (2007). Optical fiber vibration and acceleration model, *2007 IEEE International Frequency Control Symposium Jointly with the 21st European Frequency and Time Forum*, pp. 547-551, Geneva, Switzerland, 29 May–1 June, 2007
- Bloch, M; Mancini, O. & Stone, C. (2005). Method for achieving highly reproducible acceleration insensitive quartz crystal oscillators, *U.S. Patent 07106143*, 2006

- Driscoll, M.M. (1993). Reduction of Quartz Oscillator flicker-of-frequency and white phase noise (floor) levels of acceleration sensitivity via use of multiple resonators. *IEEE Transactions on Ultrasonics, Ferroelectrics, and Frequency Control*, Vol. 40, No.4, pp. 427-430, July 1993
- Driscoll, M.M. & Donovan, J.B. (2007). Vibration-Induced Phase Noise: It Isn't Just About the Oscillator, *Proceedings of 2007 IEEE International Frequency Control Symposium Jointly with the 21st European Frequency and Time Forum*, pp. 535-540, Geneva, Switzerland, 29 May-1 June, 2007
- Eliyahu, D.; Seidel, D. & Maleki, L. (2008). RF amplitude and phase-noise reduction of an optical link and an opto-electronic oscillator. *IEEE Transactions on Microwave Theory and Techniques*, Vol. 56, No. 2, pp. 449-456, February 2008
- Filler, R.L.; Kosinski, J.A. & Vig, J.R. (1983). Further Studies on the Acceleration Sensitivity of Quartz Resonators, *Proceedings of 37th Annual Symposium on Frequency Control*, pp. 265 - 271, 1983
- Filler, R.L. (1988). The acceleration sensitivity of quartz crystal oscillators: A review. *IEEE Transactions on Ultrasonics, Ferroelectrics, and Frequency Control*, Vol. 35, No. 3, pp. 297-305, May 1988
- Foreman, S.M; Ludlow, A.D; Miranda, M.H.G.; Stalnaker, J. E.; Diddams, S.A. & Ye, J. (2007). Coherent optical phase transfer over a 32-km fiber with 1 s instability at 10^{-17} . *Physical Review Letter*, Vol. 99, pp. 153601 (4), October 2007
- Fruehauf, H. (2007). "g"-Compensated, Miniature, High Performance Quartz Crystal Oscillators, http://www.frequelec.com/tech_lit.html, April 2007.
- Grove, J.; Hein, J.; Retta, J.; Schweiger, P.; Solbrig, W. & Stein, S.R. (2004). Direct-digital phase-noise measurement, *Proceedings of the 2004 IEEE International Frequency Control Symposium and Exposition*, pp. 287 - 291, 23-27, August 2004
- Hati, A.; Howe, D.A. & Nelson, C.W. (2006). Comparison of AM noise in commercial amplifiers and oscillators at X-band, *Proceedings of 2006 IEEE International Frequency Control Symposium*, pp. 740-744, June 2006
- Hati, A.; Nelson, C.W; Howe, D.A.; Ashby, N.; Taylor, J., Hudek, K.M.; Hay, C.; Seidel, D.J. & Eliyahu, D. (2007). Vibration sensitivity of microwave components, *Proceedings of 2007 IEEE International Frequency Control Symposium Jointly with the 21st European Frequency and Time Forum*, pp. 541-546, Geneva, Switzerland, 29 May-1 June, 2007
- Hati, A.; Nelson, C.W.; Taylor, J.; Ashby, N. & Howe, D.A. (2008). Cancellation of Vibration-Induced Phase Noise in Optical Fibers. *IEEE Photonics Technology Letters*, Accepted for future publication, 2008
- Hay, C.E.; Harrell, M.E. & Kansy, R.J. (2004). 2.4 and 2.5 GHz miniature, low-noise oscillators using surface transverse wave resonators and a SiGe sustaining amplifier, *Proceedings of the 2004 IEEE International Frequency Control Symposium and Exposition*, pp. 174 - 179, 23-27 August 2004
- Healy, D.J.; Hahn, H. & Powell, S. (1983). A measurement technique for determination of frequency vs. acceleration characteristics of quartz crystal units, *Proceedings of the 37th Annual Symposium on Frequency Control*, pp. 284-289, 1983
- Howe, D.A.; Lanfranchi, J.; Cutsinger, L.; Hati, A. & Nelson, C.W. (2005). Vibration-induced PM noise in oscillators and measurements of correlation with vibration sensors, *Proceedings of the 2005 IEEE International Frequency Control Symposium and Exposition*, pp. 494-498, 29-31 August, 2005

- Howe, D.A.; Hati, A.; Nelson, C.W.; Taylor, J. & Ashby, N. (2007). Active vibration-induced PM noise control in optical fibers: preliminary studies, *2007 IEEE International Frequency Control Symposium Jointly with the 21st European Frequency and Time Forum*, pp. 552-556, Geneva, Switzerland, 29 May-1 June, 2007
- Huang, S.; Tu, M.; Yao, S. & Maleki, L. (2000). A turnkey optoelectronic oscillator with low acceleration sensitivity, *Proceedings of the 2000 IEEE/EIA International Frequency Control Symposium and Exhibition*, pp. 269-279, 2000
- Kadiwar R.K & Giles, I.P. (1989). Optical fibre Brillouin ring laser gyroscope. *Electronics Letters*, Vol. 25, No. 25, pp. 1729 - 1731, 1989
- Kosinski, J. A. (2000). Theory and design of crystal oscillators immune to acceleration: Present state of the art, *Proceedings of the 2000 IEEE/EIA International Frequency Control Symposium and Exhibition*, pp. 260-268, 2000.
- Kwon, T.M. & Hahn, T. (1983). Improved vibration performance in passive atomic frequency standards by servo-loop control, *Proceedings of the 37th Annual Symposium on frequency control*, pp. 28-20, 1983
- Lance, A.L.; Seal, W.D. & Labaar, F. (1984). Phase noise and AM noise measurements in the frequency domain. *Infrared and Millimeter Waves*, Vol. 11, pp. 239-289, 1984
- Leeson, D.B. (1966). A simple model of feed back oscillator noise spectrum, *Proceeding of the IEEE*, Vol. 54, No. 2, pp. 329-330, 1966
- Mancini, O. (2004). Tutorial on Precision Frequency Generation, *Microwave Theory & Techniques Society of the IEEE Long Island Section*, 18 March 2004. http://www.ieee.li/pdf/viewgraphs_freq.pdf
- Minasian, R. (2006). Photonic signal processing of microwave signals. *IEEE Transactions on Microwave Theory and Technology*, Vol. 54, No. 2, pp. 832-846, February 2006
- Parker, T.E. & Montress, G.K. (1988). Precision surface-acoustic-wave (SAW) oscillators. *IEEE Transactions on Ultrasonics, Ferroelectrics, and Frequency Control*, Vol. 35, No. 3, pp. 342 - 364, May 1988
- Renoult, P.; Girardet, E. & Bidart, L. (1989). Mechanical and acoustic effects in low phase noise piezoelectric oscillators, *Proceeding of the 43rd Annual Symposium on Frequency Control*, pp. 439-446, 31 May-2 June, 1989
- Riley, W. (1992). The Physics of the environmental sensitivity of rubidium gas cell atomic Frequency standards. *IEEE Transactions on Ultrasonics, Ferroelectrics, and Frequency Control*, Vol. 39, pp. 232-240, 1992
- Römisch, S.; Kitching, J.; Ferre-Pikal, E.S.; Hollberg L. & Walls, F.L. (2000). Performance evaluation of an optoelectronic oscillator. *IEEE Transactions on Ultrasonics, Ferroelectrics, and Frequency Control*, Vol. 47, pp. 1159-1165, September 2000
- Rosati V.J. & Filler, R. L. (1981). Reduction of the effects of vibration on SC-cut quartz crystal oscillators, *Proceedings of the 35th Annual Symposium on Frequency Control*, pp. 117-121, 1981
- Rubiola, E.; Salik, E.; Huang, S.; Yu, N. & Maleki, L. (2005). Photonic delay technique for PM noise measurement of microwave oscillators. *Journal Optical Society of America B: Optical Physics*, Vol. 22, No.5, pp. 987-997, May 2005
- Steinberg, D.S. (2000). *Vibration Analysis for Electronic Equipment*, John Wiley & Sons, Inc. 9780471376859, NY, USA

- Sullivan, D.B; Allan, D.W.; Howe, D.A. & Walls F. L. (1990). Characterization of clocks and oscillators. *National Institute of Standards and Technology Technical Note 1337*, Section A-6, March 1990
- Taylor, J.; Nelson, C.W.; Hati, A.; Ashby, N. & Howe, D.A. (2008). Vibration-induced PM noise measurements of a rigid optical fiber spool, *Proceedings of the 2008 IEEE International Frequency Control Symposium*, pp. 807-810, Hawaii, May 2008
- Thieme, B., Zoschg, D. & Baister, G. (2004). Space worthy electronics package for the 35kg space active hydrogen maser on ACES, *18th European Frequency and Time Forum*, April 2004
- Vig, J.R.; Audoin, C.; Cutler, L.S.; Driscoll, M.M.; EerNisse, E.P.; Filler, R.L.; Garvey, R.M.; Riley, W.L.; Smythe, R.C. & Weglein, R.D. (1992). Acceleration, vibration and shock effects-IEEE standards project P1193, *Proceedings of the 46rd Annual. Symposium on Frequency Control*, pp. 763-781, 1992
- Wallin, T.; Josefsson, L. & Loftner, B. (2003). Phase noise performance of sapphire microwave oscillators in airborne radar systems, *GigaHertz 2003. Proceedings from the Seventh Symposium*, Linköping, Sweden, November 4-5, 2003
- Walls, F.L. & Ferre-Pikal, E.S. (1999). Measurement of frequency, phase noise and amplitude noise. *Wiley Encyclopedia of Electrical and Electronics Engineering*, Vol. 12, pp. 459-473, June 1999
- Watts, M.H.; EerNisse, E.P.; Ward, R.W. & Wiggins, R.B. (1988). Technique for measuring the acceleration sensitivity of SC-cut quartz resonators, *Proceedings of the 42rd Annual Symposium on Frequency Control*, pp. 442-446, 1988
- Weglein, R.D. (1989). The vibration-induced phase noise of a visco-elastically supported crystal resonator, *Proceedings of the 43rd Annual Symposium on Frequency Control*, pp. 433-438, 1989
- Yao, X.S. & Maleki, L. (1996). Optoelectronic microwave oscillator. *Journal Optical Society of America B*, Vol. 13, No.8, pp. 1725-1735, 1996